Backbone folding of the polypeptide cardiac stimulant anthopleurin-A determined by nuclear magnetic resonance, distance geometry and molecular dynamics

Andrew E. Torda, Bridget C. Mabbutt, Wilfred F. van Gunsteren[+] and Raymond S. Norton

School of Biochemistry, University of New South Wales, Kensington, NSW 2033, Australia and
[+]*Laboratory of Physical Chemistry, University of Groningen, Nijenborgh 16, 9747 AG, Groningen, The Netherlands*

The solution conformation of the cardiac stimulatory sea anemone polypeptide anthopleurin-A has been characterised using distance geometry and restrained molecular dynamics calculations. A set of 253 approximate interproton distance restraints and 14 peptide backbone torsion angle restraints derived from two-dimensional ^{1}H-NMR spectra at 500 MHz were used as input for these calculations. 13 structures generated by either metric matrix or variable target function distance geometry calculations were refined using energy minimisation and restrained molecular dynamics. The resulting structures contain a region of twisted antiparellel β-sheet to which two separate regions of unordered chain are linked by three disulphide bonds. Two loops, one including Pro-41 and the other encompassing residues 10–18, are poorly defined by the NOE data.

Polypeptide; Three-dimensional structure; ^{1}H-NMR; NOE; Distance geometry; Molecular dynamics

1. INTRODUCTION

The northern Pacific sea anemone *Anthopleura xanthogrammica* produces as part of its nematocyst venom a polypeptide of M_r ~5100 which exerts marked effects on excitable tissues [1]. This molecule, anthopleurin-A, is a potent cardiac stimulant, producing a positive inotropic response in vitro at nanomolar concentrations [2]. Its activity is not associated with any significant effects on heart rate or blood pressure in vivo [3,4], making it a valuable lead in the development of new therapeutic agents for treatment of congestive

heart failure and cardiac arrhythmias.

We have undertaken a study of the structure of AP-A in solution, commencing with ^{13}C NMR [5,6] and continuing more recently with ^{1}H NMR. The latter has provided information on the presence of conformational heterogeneity in AP-A [7], the pK_a values of its ionisable residues [8] and the degree of exposure of the aromatic residues [9]. Based on an incomplete set of resonance assignments made at 300 MHz [10], the main secondary structure elements of AP-A were identified as a small core of antiparallel β-sheet and at least one β-turn [11]. Recently, a more complete set of resonance assignments has been obtained at 500 MHz [12]. Using these assignments, a set of NOE values has been determined which provides the basis for elucidation of the overall structure of AP-A in solution by a combined approach involving distance geometry [13,14] and restrained molecular dynamics [15,16] calculations, as described in this paper.

Correspondence address: R.S. Norton, School of Biochemistry, University of New South Wales, Kensington, NSW 2033, Australia

Abbreviations: AP-A, anthopleurin-A; NOE, nuclear Overhauser enhancement; NOESY, two-dimensional nuclear Overhauser enhancement spectroscopy; RMSD, root mean square difference

2. MATERIALS AND METHODS

The NOE values used as constraints in the structure determination were obtained from NOESY spectra of 10 mM AP-A in ^2H_2O or 90% $H_2O/10\%$ ^2H_2O (v/v), recorded at 500 MHz with phase-sensitive detection as described elsewhere [12]. Distance geometry calculations were carried out using either the metric matrix approach implemented in the program DISGEO [13] or the variable target function approach utilised in the program DISMAN [14]. DISGEO calculations were carried out on a VAX 8350, DISMAN on an IBM 3090-180E. All energy minimisation and restrained molecular dynamics calculations were performed on the IBM using the GROMOS-87 suite of programs [17]. These programs were also used for numerical analysis and comparison of the structures. Structures were displayed using the program Chem-X, from Chemical Design Ltd., Oxford.

3. RESULTS

Initially a set of 251 NOE values, comprising 150 intra-residue, 61 sequential and 40 medium- and long-range ($i-j \geq 2$) constraints was derived from NOESY spectra. These NOEs were classified as strong, medium or weak on the basis of cross-peak intensities in NOESY spectra, and were assigned upper limits [13,14,16] of 0.25, 0.30 and 0.42 nm, respectively, by comparison with cross-peaks between protons at fixed distances around the three Trp rings in AP-A. In addition to these distance constraints, 13 dihedral angle constraints were included based on the calibration curve between $^3J_{NH-H\alpha}$ and the angle ϕ [18]. These angles were set at $-120°$ for coupling constants ≥ 9.0 Hz (measured from one-dimensional spectra).

These distance and angle constraints were then used as input for distance geometry calculations performed using the programs DISGEO and DISMAN. DISGEO runs were carried out essentially as described [13,19], with 10 substructures being embedded and half of these selected for full matrix embedding. A total of 26 structures was generated using DISMAN, as described [14]. Energy minimisation was then performed on these structures by subjecting each to 500 cycles of steepest descent minimisation using a force field containing both distance and dihedral restraint terms. The 13 structures with the lowest sum of distance restraint violations were then refined by restrained molecular dynamics simulations conducted in vacuo with weak coupling to a constant

temperature bath. Briefly, the protocol for these simulations was as follows: 3 ps at 300 K with K_{dc} (the force constant for the distance restraints term) set to 200 kJ·mol⁻¹·nm⁻², 2 ps at 1000 K with K_{dc} 1000, then 10 ps at 1000 K, 3 ps at 600 K and 14 ps at 300 K, all with K_{dc} 1500. The force constant for dihedral angle restraints, K_{dlr}, was held at 70 kJ·mol⁻¹ throughout the simulations.

Disulphide bonds were incorporated in the distance geometry calculations by inclusion of the SS and C^βSS distances as constraints. In the restrained molecular dynamics and energy minimisation calculations they were treated as covalent bonds. Strong long-range $C^\beta H-C^\beta H$ NOEs were observed across the Cys-4—Cys-46 and Cys-29—Cys-47 disulphide bonds, consistent with the cysteine pairings determined chemically [1].

At this stage in the structure determination a further two NOE restraints (one long-range and one sequential) and one angle restraint ($^3J_{NH-H\alpha} < 5.0$ Hz, corresponding to ϕ $-65°$ [18]) were included. The 11 best structures derived from the MD simulations described above (chosen by the criterion of total distance restraint violations after energy minimisation) were then refined by incorporating these additional restraints in further simulations carried out as follows: 1 ps at 600 K, 5 ps cooling to 300 K, 3 ps at 300 K (all with K_{dc} 1500). To consider time-averaged properties, a 20 ps trajectory was run for each of these structures at 300 K, with a configuration saved every 2 ps. The final structures were then subjected to energy minimisation. Full details of the protocols used in these structure determinations will be published elsewhere.

The eight best structures, as judged by the criterion of smallest total distance restraint violations, are documented in table 1. All structures have low total potential energies, with only small contributions arising from violations of distance and dihedral angle restraints. The dihedral angle restraints were satisfied to within 20° or better in all cases.

An evaluation of the distance restraints and dihedral angle restraints used in generating these structures indicated that most of them were associated with a region of AP-A consisting of the distorted four-strand antiparallel β-sheet identified previously [11], together with reverse turns and the three disulphide bonds. This region of the

Table 1

Properties of AP-A structures determined by distance geometry and restrained molecular dynamics[a]

Structure[b]	Violations[c]		Energy $(kJ \cdot mol^{-1})^{d}$			RMSD[c] vs average[e]	
	Σ dc (nm)	No.	E_{pot}	E_{dc}	E_{dir}	Defined $C^{\alpha f}$	C^{α}
DM1	1.02	33	−2122	52	33	0.18	0.31
DG1	1.06	29	−2145	57	31	0.18	0.31
DG2	1.10	27	−2241	55	26	0.18	0.32
DG3	1.32	31	−2171	72	32	0.26	0.38
DM2	1.51	29	−1977	114	30	0.24	0.34
DM3	1.53	30	−2024	111	40	0.23	0.45
DG4	1.57	33	−2213	93	40	0.32	0.46
DM4	1.64	32	−2159	114	32	0.24	0.38

[a] Structures are listed in order of the sum of distance restraint violations Σ dc. The rank order obtained using this criterion is similar to that which would be obtained using E_{dc}, the energy associated with the distance restraint violations, as a criterion

[b] Structures derived from DISMAN are denoted DMn, those from DISGEO DGn. All data in this table refer to structures refined by restrained molecular dynamics simulations as described in the text

[c] For each structure, violations and root mean square differences (in nm) were obtained from the average of ten structures generated at 2 ps intervals during 20 ps of averaging at 300 K with K_{dc} 1500 $kJ \cdot mol^{-1} \cdot nm^{-2}$ and K_{dir} 10 $kJ \cdot mol^{-1}$

[d] Obtained after energy minimisation of structures subjected to 20 ps of averaging as described in footnote [c]. E_{dir} is the energy associated with the dihedral angle restraints

[e] RMSD vs average over eight structures included in this table

[f] C^{α} atoms of the following 27 residues: 2–7, 20–25, 29–30, 33–38 and 44–49
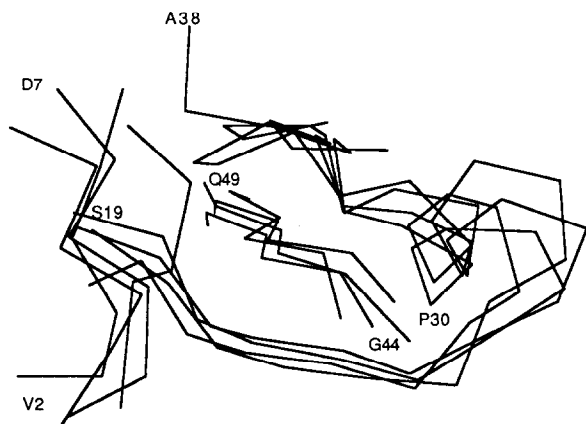

Fig.1. Comparison of the backbone C^{α} atoms of the defined regions (cf. table 1) in the four best structures of AP-A from table 1.

molecule, encompassing residues 2–7, 20–38 and 44–49, is thus much more precisely defined than the remainder of the polypeptide backbone, as in-

dicated by the two sets of root mean square differences shown in table 1. The backbone C^{α} atoms of the well-defined regions in the four best structures are shown in fig.1, while in fig.2a stereo view of the entire backbone is shown for one of the best structures (DM1 in table 1).

In keeping with most other protein structures determined to date from ^{1}H NMR data, the side-chains in our structures are not as well defined as the backbone. The side-chains of Trp-23 and -33 and several surrounding residues, including Thr-21, are, however, constrained by a number of inter-residue NOEs. As this region of the structure has been found to be conserved in homologous polypeptides from the anemone *Anemonia sulcata* [20] and to constitute a small hydrophobic patch on the surface of these polypeptides [9], the relative orientation of these side-chains in the best four structures is shown in fig.3.
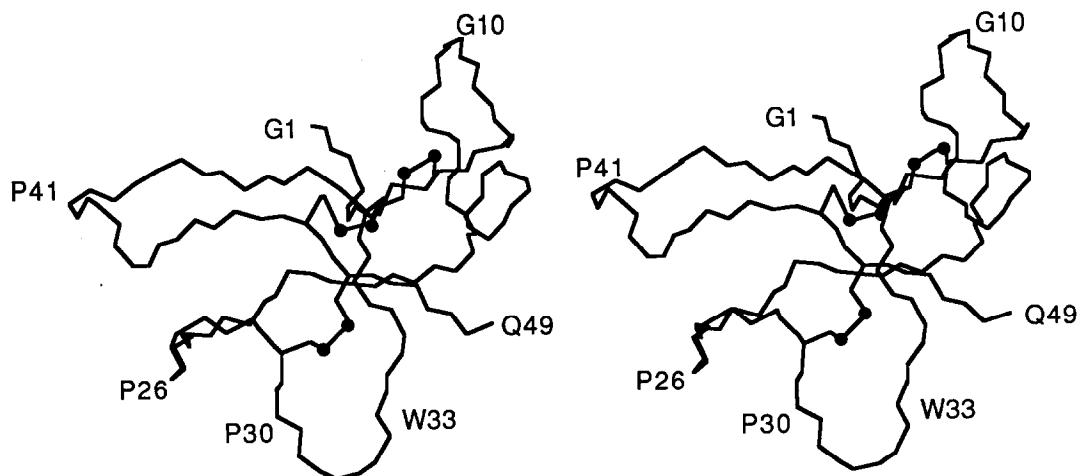
Fig.2. Stereo view of the backbone conformation of the structure DM1, which showed the lowest total distance restraint violation. Backbone heavy atoms and disulphide bonds are shown.
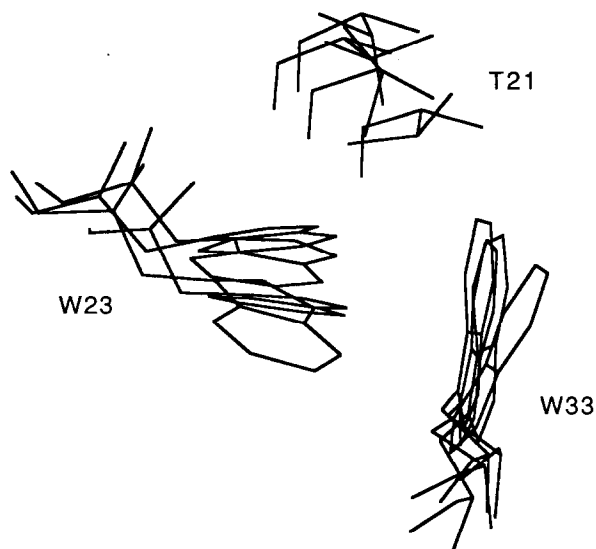

Fig.3. Sidechain orientations of Thr-21, Trp-23 and Trp-33 in the four best structures of AP-A listed in table 1. Fitting was performed on the heavy atoms of these three side-chains.

4. DISCUSSION

In this work we have obtained a family of closely related structures for AP-A which are of low potential energy and which largely satisfy the distance and dihedral angle restraints derived from

^{1}H NMR data. The final structures were generated by restrained molecular dynamics refinement of a family of structures derived from distance geometry calculations. The refined structures were of lower overall energy than those obtained by simple energy minimisation of the distance geometry structures, and showed fewer significant violations of the experimental restraints. It is noteworthy that structures derived from the two different distance geometry programs DISGEO and DISMAN are equally represented in the best eight structures following molecular dynamics refinement.

The structures contain a core of distorted antiparallel β-sheet to which the three disulphide bonds are connected, as well as a β-turn involving residues 30–33 and a less well-defined turn in the region of residues 25–28. There are two loops, one involving residues 37–43 and the other residues 10–18, that are poorly defined in the structures as a result of a lack of long-range NOEs to other parts of the molecule. The first of these loops contains Pro-41, *cis-trans* isomerism of which has been suggested to be the origin of the conformational heterogeneity observed in AP-A [7,8]. The second contains Arg-14, which appears to be essential for activity ([21] and Gould, A.R. et al., to be submitted).

It is not clear if these two loops have greater mobility than the better defined regions of the

structure. ^{1}H NMR relaxation measurements on AP-A have been used to estimate rotational correlation times for Thr-17 and Thr-42, with the result that the apparent rates of molecular reorientation calculated for these residues are very similar to those for residues in the β-sheet [22]. It is possible that additional motions do occur, but on a time scale not detected by the relaxation measurements. In any case it is likely that the Arg-14 containing loop can undergo conformational changes upon binding to the sodium channel, as it has few close contacts with other regions of the molecule that might be expected to constrain its structure. Further work on AP-A will therefore address the structure of this loop not only in un-complexed AP-A in solution, but also in the receptor-bound form of the molecule.

REFERENCES

[1] Norton, T.R. (1981) Fed. Proc. 40, 21–25.

[2] Shibata, S., Norton, T.R., Izumi, T., Matsuo, T. and Katsuki, S. (1976) J. Pharmacol. Exp. Ther. 199, 298–309.

[3] Blair, R.W., Peterson, D.F. and Bishop, V.S. (1978) J. Pharmacol. Exp. Ther. 207, 271–276.

[4] Scriabine, A., Van Arman, C.G., Morgan, G., Morris, A.A., Bennett, C.D. and Bohidar, N.R. (1979) J. Cardiovasc. Pharmacol. 1, 571–583.

[5] Norton, R.S. and Norton, T.R. (1979) J. Biol. Chem. 254, 10220–10226.

[6] Norton, R.S., Norton, T.R., Sleigh, R.W. and Bishop, D.G. (1982) Arch. Biochem. Biophys. 213, 87–97.

[7] Gooley, P.R., Blunt, J.W. and Norton, R.S. (1984) FEBS Lett. 174, 15–19.

[8] Gooley, P.R., Blunt, J.W., Beress, L. and Norton, R.S. (1988) Biopolymers 27, 1143–1157.

[9] Norton, R.S., Beress, L., Stob, S., Boelens, R. and Kaptein, R. (1986) Eur. J. Biochem. 157, 343–346.

[10] Gooley, P.R. and Norton, R.S. (1985) Eur. J. Biochem. 153, 529–539.

[11] Gooley, P.R. and Norton, R.S. (1986) Biochemistry 25, 2349–2356.

[12] Mabbutt, B.C. and Norton, R.S. (1988) submitted.

[13] Havel, T.F. and Wüthrich, K. (1985) J. Mol. Biol. 182, 281–294.

[14] Braun, W. and Go, N. (1985) J. Mol. Biol. 186, 611–626.

[15] Zuiderweg, E.R.P., Scheek, R.M., Boelens, R., Van Gunsteren, W.F. and Kaptein, R. (1985) Biochimie 67, 707–715.

[16] Clore, G.M., Nilges, M., Brünger, A.T., Karplus, M. and Gronenborn, A.M. (1987) FEBS Lett. 213, 269–277.

[17] Van Gunsteren, W.F. and Berendsen, H.J.C. (1987) GROMOS Manual, Biomos, Groningen.

[18] Pardi, A., Billeter, M. and Wüthrich, K. (1984) J. Mol. Biol. 180, 741–751.

[19] Wagner, G., Braun, W., Havel, T.F., Schaumann, T., Go, N. and Wüthrich, K. (1987) J. Mol. Biol. 196, 611–639.

[20] Gooley, P.R., Blunt, J.W., Beress, L., Norton, T.R. and Norton, R.S. (1986) J. Biol. Chem. 261, 1536–1541.

[21] Barhanin, J., Hugues, M., Schweitz, H., Vincent, J.-P. and Lazdunski, M. (1981) J. Biol. Chem. 256, 5764–5769.

[22] Torda, A.E. and Norton, R.S. (1988) Biopolymers, in press.